Available online at www.sciencedirect.com
SCIENCE DIRECT®
Biomaterials 26 (2005) 6836–6845
Biomaterials
www.elsevier.com/locate/biomaterials

# Tuning compliance of nanoscale polyelectrolyte multilayers to modulate cell adhesion

Michael T. Thompson[a,c], Michael C. Berg[b], Irene S. Tobias[a], Michael F. Rubner[a], Krystyn J. Van Vliet[a,*]

[a]*Department of Materials Science and Engineering, Massachusetts Institute of Technology, 77 Massachusetts Avenue, Cambridge, MA 02139, USA*
[b]*Department of Chemical Engineering, Massachusetts Institute of Technology, 77 Massachusetts Avenue, Cambridge, MA 02139, USA*
[c]*Harvard-MIT Division of Health Sciences and Technology, Massachusetts Institute of Technology, 77 Massachusetts Avenue, Cambridge, MA 02139, USA*

Received 11 January 2005; accepted 3 May 2005
Available online 21 June 2005

**Abstract**

It is well known that mechanical stimuli induce cellular responses ranging from morphological reorganization to mineral secretion, and that mechanical stimulation through modulation of the mechanical properties of cell substrata affects cell function in vitro and in vivo. However, there are few approaches by which the mechanical compliance of the substrata to which cells adhere and grow can be determined quantitatively and varied independent of substrata chemical composition. General methods by which mechanical state can be quantified and modulated at the cell population level are critical to understanding and engineering materials that promote and maintain cell phenotype for applications such as vascular tissue constructs. Here, we apply contact mechanics of nanoindentation to measure the mechanical compliance of weak polyelectrolyte multilayers (PEMs) of nanoscale thickness, and explore the effects of this tunable compliance for cell substrata applications. We show that the nominal elastic moduli $E_s$ of these substrata depend directly on the pH at which the PEMs are assembled, and can be varied over several orders of magnitude for given polycation/polyanion pairs. Further, we demonstrate that the attachment and proliferation of human microvascular endothelial cells (MVECs) can be regulated through independent changes in the compliance and terminal polyion layer of these PEM substrata. These data indicate that substrate mechanical compliance is a strong determinant of cell fate, and that PEMs of nanoscale thickness provide a valuable tool to vary the external mechanical environment of cells independently of chemical stimuli.


*Keywords:* Cell adhesion; Stress analysis; Endothelial cells; Atomic force microscopy; Polyelectrolyte multilayers

## 1. Introduction

The living, eukaryotic cell is an intricate sensor and actuator, responding dramatically to minute changes in external mechanical and biochemical environments. Vascular endothelial cells represent one important cell type which responds to both fluid flow-induced monotonic shear stress [1,2] and substrate-mediated cyclic radial stress [3] through morphological reorganization and, ultimately, changes in phenotype or function. A distinct but important approach to the mechanical modulation of cell function is through manipulation of the mechanical properties of the underlying substrate, as is critical in the development of tissue engineering scaffolds.

The mechanical compliance of cell substrata affects acquisition of specific cell functions in vivo and in vitro. For example, in vivo studies have shown that cardiac trauma concurrent with significant local decreases in cardiac tissue compliance can cause smooth muscle cells to secrete bone minerals typically produced by

*Corresponding author. Tel.: +1 617 253 3315; fax: +1 617 253 8745.
*E-mail address:* krystyn@mit.edu (K.J. Van Vliet).
*URL:* http://web.mit.edu/vvgroup.

0142-9612/$ - see front matter © 2005 Elsevier Ltd. All rights reserved.
doi:10.1016/j.biomaterials.2005.05.003

osteoblasts [4]. Additionally, in vitro studies have shown that the motility of and contractile forces generated by fibroblasts, the chief cellular components of scar tissue, can be directed by varying the nominal mechanical compliance of the underlying poly(acrylamide)-based bulk hydrogel substrata [5]. However, as it is well known that soluble and substrata-bound biochemicals also strongly affect cell function, it has been difficult to decouple the mechanical and chemical cues of cell response within a single experimental system. This complexity is due chiefly to two factors: (1) There are few materials which can be assembled to vary mechanical properties over a significant range without significant modulation of the polymer chemistry, e.g., addition of chemical crosslinking agents; (2) there exist few approaches to quantify the mechanical properties of such materials within aqueous environments that parallel in vitro conditions. Indeed, our limited capacity to deconvolute effects of mechanical and biochemical stimuli on cell phenotype is underscored by the introduction of combinatorial chemistry approaches whereby hundreds of distinct biopolymer compositions are rapidly screened to identify a suitable substrates for directed stem cell differentiation [6].

In this study, we utilize a unique substrata material system, weak polyelectrolyte multilayers (PEMs), and show that the PEM mechanical properties can be controlled directly through modulation of the component solution pH during PEM assembly. Polyelectrolyte multilayers are named as such due to the layer-by-layer (LbL) method of assembly, and are in fact interpenetrating networks rather than mesoscopic/macroscopic layers. These materials naturally form ionic crosslinks between polyanions and polycations during PEM assembly. The degree of ionic crosslinking for a given polyanion/polycation pair increases as assembly pH approaches neutrality. Thus, the extent to which the PEM swells in aqueous environments decreases as assembly pH approaches neutrality. Nanoscale poly(acrylic acid)/poly(allyl amine hydrochloride) PAA/PAH PEM films (thickness $h < 50$ nm) have been reported previously to affect fibroblast and hepatocyte adhesion as a function of assembly pH and in proportion to PEM swellability [7–9]. Although the extent to which PEMs swell would be expected intuitively to scale with the mechanical compliance of the polymer, systematic mechanical characterization of adhered, hydrated PEM films of thickness $<1$ μm has not been reported and thus cannot be correlated with mechanical properties of biological cell substrata. Thus, our objectives herein were to (1) characterize systematically the nominal elastic moduli $E_s$ of thin ($h \leqslant 200$ nm) PEM substrata in aqueous environments, and (2) to correlate $E_s$ with the adhesion and proliferation of human microvascular endothelial cells (MVECs) through independent variation of $E_s$ and PEM surface chemistry. The capacity to quantify local deformation of polymeric films in aqueous environments through adaptations of nanoindentation in scanning probe microscopes or SPMs [10–12] is a promising approach to such quantification, provided the complexity of multiaxial contact deformation in viscoelastoplastic substrata is considered carefully. Although SPM-enabled nanoindentation has been recently applied to estimate $E_s$ of several hydrated PEM systems of μm-scale film thickness [12–14] and of hydrated PEM microcapsules of nm-scale wall thickness [15,16], this study quantifies the nanoindentation-measured $E_s$ of hydrated, nm-scale PEMs in relation to adherent cell response.

## 2. Materials and methods

### 2.1. Assembly of weak polymer electrolyte multilayers

Poly(acrylic acid) (PAA, Polysciences), poly(acrylamide) (PAAm, Polysciences), and poly(allylamine hydrochloride) (PAH, Sigma-Aldrich), were used to assemble PAA/PAH and PAA/PAAm polyelectrolyte multilayers (PEMs) as described previously [7,8,17,18]. Briefly, dilute solutions of polyelectrolytes (0.01 M) were prepared in deionized water (Milli-Q, 18 MΩ/cm), and pH adjusted to 2.0, 4.0, or 6.5 using HCl or NaOH. A LbL dipping technique was employed to coat 35 and 60 mm-diameter tissue culture-treated polystyrene Petri dishes (TCPS, Becton Dickinson, Franklin Lakes, NJ) with alternating layers of PAA and PAH adjusted to the same pH, resulting in ionically crosslinked PEMs. PEM samples are typically described in the literature by the cation/anion pair and assembly pH for each polyelectrolyte, e.g., PAA/PAH 2.0/2.0. To be consistent with such notation and further indicate the identity of polyelectrolyte added last, we denote the terminal polyion in bold type. Thus, a PAA/PAH PEM assembled at pH = 2.0 for both polyelectrolytes with a final layer of PAA is designated as **PAA/PAH** 2.0/2.0. The number of layers was varied to obtain a uniform dry (unhydrated) thickness $h = 40$ nm. For PAA/PAH PEMs assembled at pH = 2.0, there were 20 layers or 10 bilayers, at pH = 4.0 (16 layers), and at pH = 6.5 100 layers, with one additional layer thickness for PAH-terminated PEMs [19]. Unmodified TCPS and PAA/PAAm PEM (6 layers at pH = 3.0, thermally covalently crosslinked at 95 °C for 8 h) served as established, positive and negative controls for cell attachment, respectively [18]. Hydrated PEM thickness ranged from ~60 nm (pH = 6.5) to ~200 nm (pH = 2.0), as confirmed previously through in situ ellipsometry and atomic force microscopy [8,19].

### 2.2. Cell culture, attachment and proliferation assays

Human dermal microvascular endothelial cells (MVEC, Cambrex Bioscience) were maintained at 37 °C under 5% $CO_2$ in vented T75 flasks containing endothelial basal medium (EBM-2, Clonetics) supplemented by 2% fetal bovine serum as well as growth factors and antibiotics (EGM-2, Clonetics). The osmolality and pH of this media (275 mOsm; pH 7.6) is quantitatively similar to that of 150 mM PBS (276 mOsm; pH

7.4) used in nanomechanical characterization of the substrata discussed in Section 2.3 [20]. Cells were passaged every seven days, with total media exchange every 48 h. Cells used in experiments were harvested at passages 3–5.

Cell assays were carried out in 35 mm-diameter tissue culture-treated polystyrene Petri dishes (Becton Dickinson) coated with either **PAA/PAH** or **PAA/PAH** at assembly pH = 2.0, 4.0, or 6.5 as indicated. Prior to cell seeding, all surfaces were sterilized with 70% ethanol (EtOH) in a sterile field for 1 h; UV sterilization was avoided to prevent any photo-crosslinking that might alter the mechanical compliance of the substrata.

Cells were freshly cleaved from T75 flasks through trypsinization, and directly seeded in triplicate at a cell density of 84,000 cells/35 mm-diameter dish. Total media exchange was conducted every 48 h, and digital images were acquired daily to monitor attachment and growth within a single 2 μm × 2 μm region of each sample. Cells were harvested from the PEMs at day 7 post-seeding. Each sample group was cleaved individually to ensure approximately equal duration of exposure to the trypsin/EDTA cleaving agent. Cells were stained (1 neutralized cell suspension: 1 trypan blue) prior to hemacytometric counting to assess total cell number at day 7. In order to assess the effects of mechanical compliance and terminal polyion layer on initial cell attachment and subsequent cell proliferation, we determined cell density as a function of days in culture through inverted optical light microscopy (OM200, Leica) digital image acquisition and analysis of the same 6.25 $mm^2$ section of the PEM samples every 24 h up to day 6.

### 2.3. Nanoindentation of PAA/PAH multilayers

Nanoindentation of PAA/PAH multilayers assembled in 60 mm-diameter polystyrene Petri dishes was conducted using a commercially available scanning probe microscope (Molecular Force Probe 3D, Asylum Research, Santa Barbara, CA). Unsharpened silicon nitride cantilever of nominal spring constant $k_c = 0.1$ N/m and nominal probe radius of 50 nm (MHCT-AUHW, Veeco Metrology Group, Sunnyvale, CA) were used to obtain the continuous force–displacement response of the PEMs in fluid, and silicon cantilevers of nominal $k_c = 0.7-3.8$N/m and probe radius of 50 nm (AC-240, Olympus) were used to obtain the response on comparably rigid polystyrene. As the actual spring constant of each cantilever can vary significantly from nominal values reported by the manufacturer, $k_c$ was determined experimentally for each lever immediately prior to indentation as follows (see Fig. 1A). First, cantilever free end-deflection $\delta$ was calibrated as a function of laser-photodiode voltage $V$ through displacement of the cantilever against a rigid (glass or polystyrene) substrate, such that there was a 1:1 correspondence between the downward displacement of the piezo-actuated cantilever base and the upward displacement of the probe at the free end of the cantilever. Second, $\delta$ was recorded under thermal (room temperature) activation, and the Fourier transform (FFT) of cantilever amplitude as a function of oscillation frequency was fitted with the simple harmonic oscillator equation to determine $k_c$ [21]. This thermal power spectral density method is semi-automated within the instrument used herein. Experimentally determined values of $k_c$ were

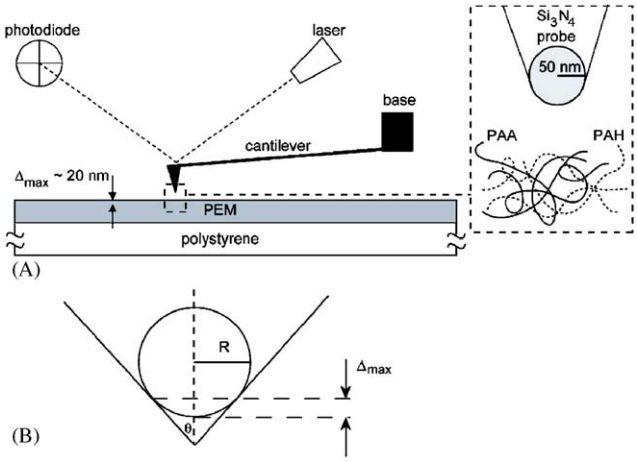


Fig. 1. Schematic of experimental system. (A) A scanning probe microscope actuates and records cantilevered probe deflection through a laser photodiode–piezoactuation feedback loop, enabling force–displacement responses to be acquired on the polymer surface in fluid. The polyelectrolyte multilayer is most accurately represented as an interpenetrating network (inset). (B) The depth to which the truncated cone can be considered a sphere can be estimated through geometry.

implemented in subsequent data analysis, and did not exceed nominal values by more than 200%.

The experimental system was allowed to achieve thermal equilibration for a minimum of 1 h inside of a customized acoustic isolation enclosure (Herzan, Inc.) prior to cantilever calibration and mechanical testing of the PEMs. This equilibration time was found necessary to minimize thermal drift of the laser-photodiode feedback response used to monitor the force–displacement response of the PEMs. Force–displacement ($P-\Delta$) responses were recorded in fluid (filtered 150 mM NaCl phosphate buffered saline; 276 mOsm, pH = 7.4) at a velocity of 2 μm/s to a maximum cantilever deflection $\delta$ of $<50$ nm. This maximum deflection, corresponding to a maximum applied force $P \leqslant 5$ nN in the PEMs, was chosen such that the resulting penetration depth $\Delta$ did not exceed the displacement over which the mechanical contact between the probe of nominally 50 nm radius and the PEM substrate could be idealized as a sphere-on-flat contact geometry (see Fig. 1B and appendix). Upon thermal equilibration of the experimental system, $P-\Delta$ responses were recorded at distinct positions on the substrate surface, such that each response was generated at a different location.

### 2.4. Analysis of nanoindentation response

Mechanical output was analyzed offline using the scientific computing software IGOR (Wavemetrics, Lake Oswego, OR). Raw experimental data includes cantilever free-end deflection $\delta$ versus cantilever base displacement $d$, and requires straightforward conversion to force versus probe penetration depth, or $P-\Delta$ responses, where

$$P = k_c\delta, \tag{1}$$

$$\Delta = d - \delta. \tag{2}$$

For purposes of analysis, we describe the polymer substrata as a sphere of radius $R_s$ and the cantilevered probe as a sphere of radius $R_p$, such that $R_s \gg R_p$. In this way, we can apply the Hertzian theory of elastic contact between spheres [22], which relates the force imposed by the cantilever $P$ to the penetration depth within the substrate $\Delta$ as,

$$P = (\tfrac{4}{3})E_r R_p^{1/2} \Delta^{3/2}, \quad (3)$$

where $R_p$ is the radius of curvature of the cantilevered probe, and $E_r$ is the reduced elastic indentation modulus comprising the elastic response of both the substrate and the probe materials. Experimentally, care was taken to acquire and analyze data within the range of indentation depth for which Hertzian analysis is reasonably valid. However, it should be noted that some loading curves showed a Hertzian elastic response beyond this estimated value of $\Delta_c$, reflecting the uncertainty to which $R_p$ is known. Eq. (3) can be represented generally as,

$$P = C\Delta^{3/2}, \quad (4)$$

where loading curvature $C$ is qualtitatively and quantitatively proportional to the elastic modulus of the indented sample $E_s$ (See Fig. 2A). Taking the logarithm of Eq. (4) yields a linear representation of the form

$$\log_{10} P = \log_{10} C + 3/2 \log_{10} \Delta = a + b \log_{10} \Delta \quad (5)$$

from which the reduced modulus $E_r$ can be calculated directly by reference to Eq. (3), as shown in Fig. 2B. The modulus of the substrata can be computed directly from $E_r$, where

$$E_r = [E_s(1-\upsilon_s^2)^{-1} + E_p(1-\upsilon_p^2)^{-1}], \quad (6)$$

where $E_s$, $\upsilon_s$ and $E_p$, $\upsilon_p$ are the Young's modulus and Poisson's ratio for the substrate material and the cantilevered probe material ($Si_3N_4$), respectively. Poisson's ratio was not measured experimentally, and was maintained fixed at a value of 0.33 and 0.45 for $Si_3N_4$ and the polymer substrata, respectively; $E_p = 310$ GPa. Here, it is equally reasonable to assume $E_p \to \infty$, such that $E_r = E_s$, with little effect on the calculated compliance. Through linear regression of the $P-\Delta$ response for $\Delta < 20$ nm, data were analyzed for each independent experiment $n$ according to Eqs. (5)–(6) to determine $E_s$. Calculated values of $E_s$ are reported as averages and standard deviations, where $n \geqslant 40$ for each sample, each a unique spatial location on the sample surface. As the above approach measures the elastic modulus of the material under multiaxial (rather than uniaxial) loading and neglects realistic polymer deformation characteristics including nonlinear elasticity and viscoelasticity, we use the term $E_s$ to represent the nominal indentation elastic modulus. This representation is related qualitatively to the Young's modulus $E$ measured through uniaxial mechanical testing of bulk, linear elastic samples.

## 3. Results

### 3.1. Effect of multilayer assembly pH on mechanical compliance

Nanoindentation of fully hydrated PAA/PAH and PAA/PAAm multilayers was conducted to quantify the mechanical compliance of these PEMs in terms of $E_s$. Fig. 3 shows that $E_s$ varies significantly as a function of assembly pH, but does not vary to a statistically significant extent as a function of the last polyelectrolyte layer added (PAA or PAH). $E_s$ increases by several orders of magnitude in direct correlation to the increase of PEM assembly pH, consistent with a model of increased interchain ionic crosslinking [19,23]. Although large deviations occur in $E_s$ values for PAA/PAH 4.0/4.0, these are indicative of the effect of thermal fluctuations during mechanical testing of hydrated polymers in fluid, and the differences among PEMs assembled at varying pH are significantly greater than this deviation. Thus, the nominal indentation elastic modulus $E_s$ of the hydrated PAA/PAH system of nm-scale thickness can be modulated significantly via the solution pH at which the multilayer is assembled, and the resulting mechanical compliance of the PEM is independent of the outermost (PAA or PAH) layer.

These PEMs are assembled under salt-free conditions in aqueous solutions, and can then be used in the hydrated state (with water or buffered salt solutions) or dried and then rehydrated for later use. Although mechanical characterization was conducted in PBS and cell assays were conducted in cell culture media, the close correspondence of osmolality and pH in these two

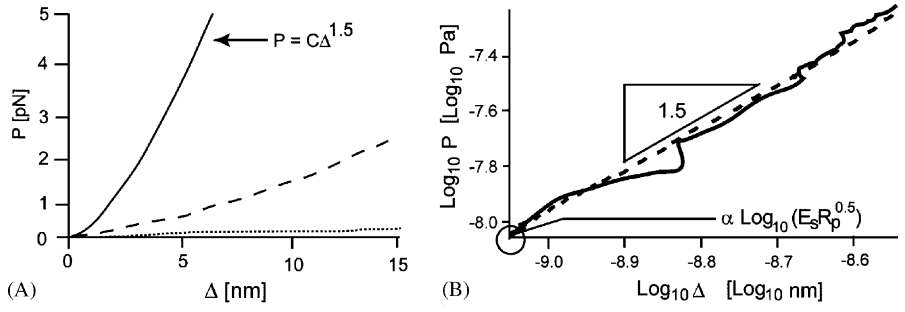


Fig. 2. (A) Representative force–displacement $P-\Delta$ responses of PEMs as a function of assembly pH (solid, pH = 6.5; dash, pH = 4.0; dot, pH = 2.0). (B) Logarithmic representation used to extract indentation modulus $E_s$.

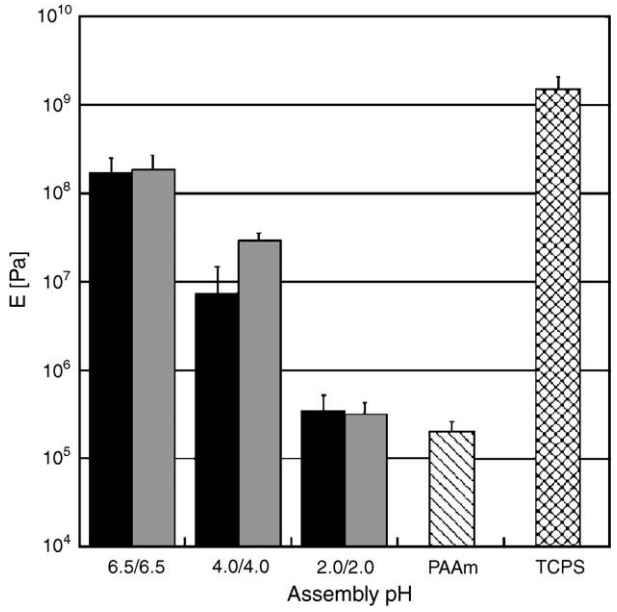


Fig. 3. Indentation elastic modulus $E_s$ as a function of assembly pH of polyanion and polycation solutions, pH = 6.5, 4.0 and 2.0. The terminal or top layer of the PEM is indicated as polyanion PAA (solid black) or polycation PAH (solid gray). Polyacrylamide multilayers (PAAm, striped) and polystyrene (TCPS, cross-hatched) are shown for reference, and used as negative and positive controls of cell attachment, respectively. Standard deviation is indicated for each sample ($n = 15$).

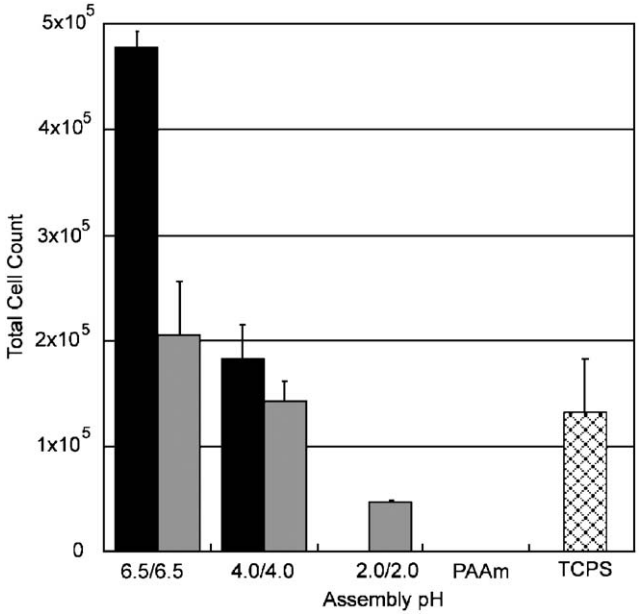


Fig. 4. Total number of cells harvested from 60 mm-diameter Petri dishes at seven days post-seeding, as a function of PEM assembly pH. The terminal or top layer of the PEM is indicated as polyanion PAA (solid black) or polycation PAH (solid gray). Polyacrylamide multilayers (PAAm) and polystyrene (TCPS) are negative and positive controls of cell attachment, respectively. Standard deviation is indicated for each sample ($n = 3$).

solutions indicates that PEM compliance will not differ with respect to solution choice. In separate studies, we have found no quantitative difference in compliance of these PEMs in PBS or cell culture media over several days in solution [24].

### 3.2. Effect of substrate compliance and assembly pH on cell attachment and proliferation

Human microvascular endothelial cells (MVECs) were cultured over a seven-day period on PAA/PAH multilayers to elucidate whether attachment and proliferation of MVECs correlated with the observed differences in mechanical compliance of the substrates. Cell density (viable cells/mm$^2$ of available substrate) at day 7 is shown in Fig. 4. A clear correlation between the cell density and $E_s$ can be observed: Cell density at day 7 post-seeding increases as the compliance of the multilayer decreases. Clearly, PEMs assembled at pH = 6.5 were the least compliant PEMs ($E_s = 153 \pm 70$ MPa) and exhibited cell densities consistent with or exceeding that of tissue culture-treated polystyrene (TCPS), regardless of the terminal polyion. Relative to the initially seeded cell population of 84,000 cells/sample, these data indicate slightly more than a single population doubling for PAH-terminal PEMs at assembly pH = 6.5; less than one population doubling for PAH-terminal PEMs at assembly pH = 4.0 (78% increase in total cell number) and TCPS (55% increase in total cell number); and a 40% decrease with respect to seeded cell number for PAH-terminal PEMs at assembly pH = 2.0. Consistent with previous reports [17], PAA/PAAm multilayers showed zero cells attached at day 7 post-seeding and were considered a negative control for cell–substratum adhesion.

Further, the differences in cell density between the PAH-terminal and PAA-terminal multilayers are quantitatively repeatable. (These data, acquired in triplicate, were confirmed through experiments conducted in duplicate; data not shown.) Although the mechanical compliance is not strongly affected by the terminal PEM layer, in general the chemical interface is altered modestly to exhibit either excess carboxylate (PAA) or excess amine (PAH) functionality of the terminal layer at near-neutral pH. That is, PAA-terminal PEMs should generally exhibit uncompensated negative surface charges at pH~7, whereas PAH-terminal PEMs should generally exhibit uncompensated positive surface charges. However, this is an oversimplification, as the amount of uncompensated surface charge is also related to the assembly pH and polycation pairs in a complex manner; we refer the reader to Ref. [19] for a detailed discussion of this point. Therefore, assembly pH of PAA/PAH PEMs modulates both mechanical compliance and cell density over extended in vitro timescales, while the terminal polyelectrolyte layer modestly affects

initial cell attachment independently of substrata mechanical compliance.

In order to assess whether the inverse correlation between substratum compliance and cells harvested via trypsination at day 7 was attributable to differences in initial cell attachment, cell proliferation, or both, a single region of each sample was observed via optical microscopy over days in culture. Fig. 5 shows MVEC density (number of cells/mm$^2$ substratum) as a function of time in vitro for a single 6.25 mm$^2$ area ($n = 3$ for each condition) for PAH-terminated PEMs. These data represent cells that appeared to be well-attached to the substrate upon agitation, and distinct from rounded or fully detached cells as assessed via optical microscopy. This quantification of cell adhesion is less rigorous than trypsinization and counting of an entire sample after a fixed number of hours in vitro, but enabled observation of the same specific region of the sample over extended time periods. At 1 day post-seeding, MVEC density was inversely related to PEM compliance, indicating that initial cell adhesion to the substratum was directly related to $E_s$. MVEC density decreased for most samples upon full media exchange at day 2 (via vacuum aspiration), due presumably to poor adhesion between the nominally attached cells and substrata (and, to a lesser extent, normal detachment during cell division) in this specific region of the sample. Note that MVEC density on PAA/PAH 6.5/6.5 did not decrease upon media exchange, indicating strong cell attachment in the observed region of the sample. The increase in MVEC density over days in vitro was not a strong function of $E_s$. That is, the number of cells observed within the same specific area of the substratum over time correlated closely with that observed upon the first full media exchange via vacuum aspiration, indicating essentially no proliferation of the cells, at least in the observed region, regardless of assembly pH. The observed regions in Fig. 5 represents $<1\%$ of the total substratum area in each sample and thus may not correlate quantitatively with population doublings demonstrated in Fig. 4. However, Fig. 5 clearly demonstrates that initial cell attachment in the observed regions increases as substrata compliance decreases, and is consistent with the proliferation trends in Fig. 4 for cells harvested at day 7. Similar trends regarding the number of cells per unit area over days in vitro were observed for PAA-terminated PEMs, which showed greater cell attachment over the course of the 7-day observation than PAH-terminated PEMs for pH $>2.0$.

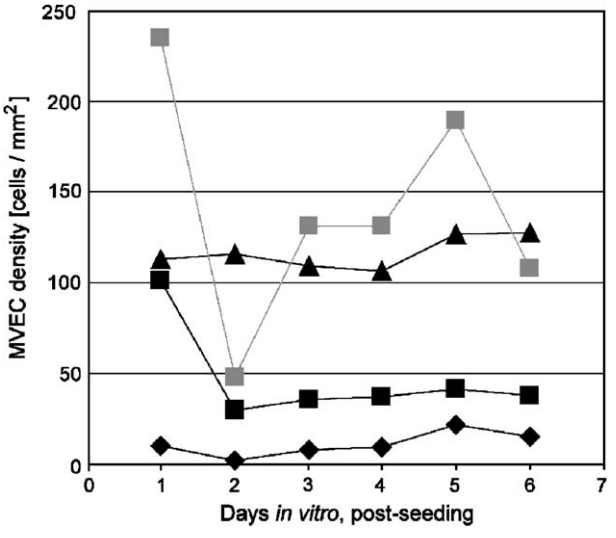


Fig. 5. Spatial density of cells attached as a function of days in culture, as measured through optical image analysis of a specific area of 6.25 mm$^2$ for each sample. PAA/PAH 2.0/2.0 (black diamond); 4.0/ 4.0 (black square); 6.5/6.5 (black triangle); and tissue culture polystyrene (gray square). Cells seeded at 84,000 cells/sample or ~30 cells/mm$^2$ if uniform density is assumed.

As noted above, we did not quantify nor control the extent of amine and carboxylic acid functional groups on the PEM surfaces as a function of terminal layers and assembly pH. Thus, these data demonstrate only that MVEC growth on these PEM substrata depends both on mechanical compliance and surface chemistry, and do not clarify how general amine/carboxylic acid functionality affects cell attachment for a given substratum compliance, as discussed below.

## 4. Discussion

The direct measurement of mechanical compliance for hydrated polyelectrolyte multilayers of nanoscale thickness in fluid allows us to correlate qualitative concepts of macromolecular structure with quantitative mechanical properties that can be compared, modulated, and correlated with cell response. For example, it is well established that the percent swelling of PAA/PAH PEMs increases as assembly pH departs from neutrality [8], yet it is difficult to characterize and design materials based upon percent swelling. However, current models hold that changes in percent swelling are a consequence of increasing or decreasing the number of ionic interchain PEM crosslinks, and it is generally known that modulation of crosslinking is a determinant of substrate compliant properties. Although the effect of these different PEM materials on cell attachment has been demonstrated previously for both fibroblasts [8] and hepatocytes [9], the approach presented herein facilitates quantitative comparison of the mechanical environment to which the cells are subjected, independent of the biochemical environment and in direct relation to other potential substratum materials such as TCPS.

### 4.1. Limits of nanoindentation experiments and analysis

Although few alternatives exist for experimentally measuring mechanical properties of hydrated polymeric

substrata of nm-scale thickness, it is important to note several limitations of this method. These limitations include idealizations of the mechanical contact problem, the finite thickness of the PEM, and the mechanical behavior of polymers.

Hertzian contact mechanics analysis is typically invoked to estimate Young's elastic modulus $E_s$ from the spherical nanoindentation response. Hertzian contact includes several assumptions regarding dimensions of the indenter and the indented material; the technical limitations of this analysis in the context of scanning probe microscope-enabled indentation are summarized in the appendix. In the present experiments, we applied this analysis by (1) idealizing the nominally sharp probe as spherical at its apex, and (2) restricting our analysis to indentation depths $\Delta < 20$ nm, the depth to which this spherical approximation would hold and to which the finite thickness of the PEM could be reasonably neglected, as discussed in the appendix. Alternatively, commercially available spherical beads for which micron-scale radii are well-known can be attached to the cantilevered probe, thus reducing the nominal stress $\sigma$ and strain $\varepsilon$ for a given $P$ while concurrently reducing the spatial resolution of the tested area [10,24]. Agreement between (film thickness-corrected) Hertzian analysis of cones and spheres result in similar magnitudes of $E_s$ for micron-scale hydrogels [12].

An equally important limitation of Hertzian analysis in the present context is that hydrated PEMs are likely best considered as viscoelastic materials over timescales relevant to cell processes, whereas we have neglected rate effects in our characterization of PEM mechanical compliance. We have confirmed that, for a fixed displacement rate of 2 μm/s and for $\Delta < \Delta_c$, neither the $P-\Delta$ response nor the calculated $E_s$ are functions of maximum load $P$. This indicates that these PEMs are linearly elastic at this loading rate and range of applied strain, but does not rule out the possibility that they are viscoelastic. We did not explore the effects of displacement rate (nominal strain rate) on the mechanical response of these PEMs. However, it is reasonable to assume that time-dependent deformation does not significantly affect cell attachment and proliferation processes that occur over a timescale of days.

Despite these constraints, it is instructive and encouraging to note that the calculated average value of $E_s$ obtained for tissue culture polystyrene, obtained without curve fitting or selective analysis of specific data sets, was ~8 GPa, which corresponds reasonably well with literature values of $E$ that range from 2.3–3.4 GPa for bulk (mm-scale thickness) polystyrene under uniaxial loading [25]. Further, Pavoor et al. have reported $E_s$ for a similar PEM system (PAA/PAH 7.5/3.5 with hydrated thickness $h = 500$ nm), as determined by instrumented nanoindentation with a sharp diamond probe [26]. This particular PEM has strongly ion-paired internal structure, much like the PAA/PAH 6.5/6.5 studied here [19]. Although the technical limitations of instrumented nanoindentation preclude analysis of significantly thinner, hydrated PEM films, these authors found $E_s = 70$ MPa, in reasonable agreement with our results for PAA/PAH 6.5/6.5 ($E_s = 150$ MPa).

Further, recently reported experiments that estimate elastic moduli for a different PEM of nm-scale thickness (sulfonated poly(styrene) SPS/PAH, $h = 20$ nm) through continuum analysis of PEM microcapsule swelling indicate $E = 130-170$ MPa [16], although AFM indentation of hydrated microcapsules indicate $E = 1.3-1.9$ GPa [15]. As both SPS and PAH are fully charged upon assembly of the SPS/PAH multilayer, this PEM is most similar to the PAA/PAH 6.5/6.5 system discussed herein. Although the microcapsule experiments differ in that the PEM microcapsule is not adhered to a rigid substrate and is deformed under osmotic pressure, these results are also consistent with our findings for PAA/PAH 6.5/6.5, and suggests that the nominal elastic properties of these nanoscale PEMs can approach those of elastomers.

In addition to the above mechanical characterization of nm-scale PEMs, others have employed SPM-enabled nanoindentation to characterize PEMs of μm-scale thickness. Although variations among PEM thickness, constituents, and assembly pH complicate direct comparison of results, μm-scale PEMs characterized in this manner over the same displacement rates appear to exhibit $E_s$ ranging $10^3$ to $10^7$ Pa, or at least two orders of magnitude more compliant than the nm-scale PAA/PAH PEMs considered in the present study. For PAH/azobenzyne-containing polyelectrolyte PEMs ($h = 1.1$ μm, pH = 5.0 to 10.5) tested in an undefined aqueous solution, Mermut et al. have reported that $E_s$ ranges 100 kPa to 10 MPa, with $E_s$ decreasing with increasing assembly pH for this polyion pairing (for pH > 5.0) [13]. Although Mermut et al. demonstrated a nonlinear decrease in $E_s$ with increasing assembly pH, $E_s$ for this PEM at pH = 6.5 can be interpolated as ~4 MPa, whereas we find $E_s$~150 MPa for nm-scale PAA/PAH PEMs assembled at pH = 6.5. For PAH/hyaluronic acid PEMs of thickness ranging 4 to 14 μm, Engler et al. have found that $E_s < 1$ MPa (ranging 40 to 300 kPa, with and without addition of a chemical crosslinker, respectively) [14]. In summary, the literature includes SPM-enabled nanoindentation measurements of chemically distinct, μm-scale PEMs that are considerably more compliant than the nm-scale weak PEMs considered here. Although it is plausible that the molecular configurations and thus mechanical properties measured at PEM surfaces may be altered over orders-of-magnitude changes in sample thickness, positive correlation of the current results with alternative measurements of $E$ in chemically similar PEMs indicates that the nature of the weak polyions and assembly

conditions—not the significantly decreased sample thickness—are chiefly responsible for the observed values of $E_s$. Systematic consideration of the effect of PEM thickness on $E_s$ measured in this manner will be reported elsewhere [24].

### 4.2. Effects of $E_s$ on cell attachment and proliferation

As $E_s$ of the PEM system herein can be modulated from $10^5$ to $10^8$ Pa for a given PEM chemistry, it is possible to consider the unique effects of substrate compliance and interfacial chemistry on MVEC attachment and proliferation. Although our results indicate that the substrata terminal layers modestly affects the initial attachment and growth of MVECs, explanation of this intriguing result based on amine/carboxylic acid surface functionality is not straightforward due to the nature of the ionic crosslinking in these PEMs. However, it is clear that mechanical compliance of the substrata affects initial cell attachment more strongly than does the ionic character of the terminal layer, in that no MVECs remained attached to the PEM substrate over seven days for compliant PAA/PAH 2.0/2.0 ($E_s$~400 kPa) for which $E_s$ was lower than that of PAA/PAH 6.5/6.5 ($E_s$~150 MPa) by several orders of magnitude. The nominal cell growth on PAA/PAH 2.0/2.0 is consistent with that observed for hepatocytes [9], and reflects the coupling between mechanical and biochemical environments in mammalian cell development.

Together, Figs. 4 and 5 indicate that MVECs attach preferentially (and, as a population, proliferate mildly but more rapidly over 7 days in vitro) on PEMs of $E_s$~150 MPa as compared to more compliant substrata (PEMs assembled at pH = 4.0 or 2.0) and less compliant substrata (TCPS). Thus, our observations are consistent with the concept that the mechanical compliance of substrata is at least as important as surface chemistry in determining whether and how cells will adhere in vitro. It should be noted that previous reports on other cell types and among various polyion combinations has demonstrated clearly that differences in cell attachment depend much more strongly on the swellability, here quantified as mechanical compliance in terms of $E_s$, than on details of PEM surface chemistry [7,8].

## 5. Conclusions

We have shown that it is possible to both measure and modulate the mechanical compliance of hydrated PEM substrata of nm-scale thickness, and to independently modulate the chemical functionality at the cell–substrate interface to regulate cell attachment and growth. Clearly, the mechanical compliance of the substrata strongly and independently affects the attachment of MVECs in vitro. Such nanoscale substrata are particularly relevant to cell studies for two reasons: The thickness and optical properties of these PEMs are amenable to advanced optical imaging approaches including epi-fluorescence. This optical imaging capability, coupled with the mechanical tunability of such thin substrata, facilitates quantitative correlation between mechanical environment and cell substructures critical to cell processes such as focal adhesion complex formation, cytoskeletal tension against the substrata, motility and phenotypic differentiation. Thus, quantitative correlation of tunable substrata mechanical compliance with cell response in these optically transparent, nm-thick materials enables future investigations of subcellular responses to mechanical cues, as well as of mechanically directed development of cell phenotypes for applications including tissue engineering.

## Acknowledgments

The authors wish to thank the DuPont–MIT Alliance and the MIT MRSEC Program of the National Science Foundation under award number DMR 02-13282 for funding, and CMSE for the generous use of shared experimental facilities supported by this MRSEC program. Additionally, MT Thompson and KJ Van Vliet acknowledge use of the MFP3D (Asylum Research, Inc.) within the MIT NanoMechanical Technology Laboratory.

## Appendix. Assumptions and technical limitations of Hertzian contact analysis

Hertzian contact mechanics enables calculation of Young's elastic modulus $E$—a mechanical property typically defined by uniaxial loading—from the multiaxial loading of a three-dimensional indenter into a sample of interest. Valid application of this model assumes several limitations regarding indenter and sample geometry, as well as the mechanical behavior of the sample. These limitations deserve particular consideration in the context of scanning probe microscope-enabled nanoindentation. Although the force and displacement resolution of the scanning probe microscope (pN and nm, respectively) are well-suited to mechanical probing of compliant materials such as synthetic biopolymers, tissues, cells and molecules, this sensitivity is due the large deflections of the compliant cantilever through which the force is applied. Because this deflection is measured through reflection of a focused laser onto a photodiode in feedback with the piezoactuated cantilever, the cantilever is inclined up to 15°, rather than parallel to the sample surface. Application of the nominally sharp, flexible probe at an angle

can induce large shear stresses and traction at the probe–surface interface, effectively sliding the probe into the surface rather than displacing normal to the surface. An additional uncertainty arises because the cantilevered probe is fabricated through mask-based etch lithography standardized within the microelectronics industry, the probe radius $R_p$ is on the order of 20–50 nm, but can vary significantly within a single wafer of fabricated cantilevers. These features of the instrument, inclination of contact loading and imperfect knowledge of the contact radius, compromise the application of Hertzian elastic contact analysis, which assumes normal loading of a sphere of known radius into a semi-infinite, elastic material. Application of this model assumes that both the probe and the substrata are linear elastic (i.e., $\varepsilon < \varepsilon_{plastic}$) and, strictly, that the substrata is semi-infinite. Neither condition is strictly true for the present case, as discussed below. Further, application of this spherical contact model requires consideration of the critical penetration depth $\Delta_c$ beyond which the nominally sharp probe is no longer well-approximated by a sphere. For the silicon nitride cantilevers used herein, with a nominal $R_2 = 50$ nm and apex half-angle of 35°, this maximum penetration depth $\Delta_{max}$ is ~20 nm, as determined from the geometry in Fig. 1B:

$$\Delta_{max} = R_p(1 - \sin\theta). \tag{A.1}$$

To mitigate the effects of these experimental realities, we determined through Eq. (A.1) that the critical penetration depth over which the probe cone radius could be considered as a sphere of $R_p = 50$ nm to $\Delta_c = 20$ nm for a cantilever inclination of 0°, and thus analyzed $P-\Delta$ responses within this range. As noted in the text, spherical probes of μm-scale radii can be and have been used to mitigate geometric uncertainties and increase the valid range of indentation depth, with an associated decrease in both spatial resolution and accuracy in identifying the point of initial loading of the sample. The latter uncertainty is due to the fact that long-range electrostatic forces are greater in magnitude and applied load $P$ increases more gradually upon approach of a charged surface such as a PEM with a larger spherical probe, even in a buffered fluid.

The finite thickness of the PEMs violates an additional assumption of Hertzian analysis, namely the semi-infinite dimensions of the indented material. It is well-known in the context of inorganic thin films that, beyond a certain ratio of indentation depth $\Delta$ to film thickness $h$, the mechanical properties of the substrate to which the film is adhered will influence the indentation response and thus the calculated $E_s$. Thus, care must be taken in the application of Hertzian contact mechanics which assumes the indented solid to be of semi-infinite thickness. For films such as metals for which the size of the elastoplastic zone of deformation in the film can be predicted analytically for a paraboloid of revolution such as a cone, $\Delta/h$ ranges from 0.1 to 0.3, depending on the relative film and substrate mechanical properties [27,28]. Dimitriadis et al. have considered this film thickness effect for spherical indentation of thin polymer films in the context of the experimental approach we employ herein, and have reported a straightforward thickness correction that idealizes the polymer as a linear elastic material [10]. This thickness correction is a polynomial function of a scaling factor:

$$\chi = (R_p\Delta)^{1/2}/h. \tag{A.2}$$

and tends toward the classical, small strain Hertzian solution of Eqs. (5)–(6) for large $h$. To attempt a relative bound on film thickness $h$ below which this correction is required for accurate calculation of $E_s$, the authors assume that the finite film thickness should perturb the $P-\Delta$ curve by at least a 10% change in $P$ and that a nominal definition of strain $\varepsilon \sim \Delta/h$ should be less than 10% to be considered sufficiently small to maintain assumptions of elastic linearity. These limits (summarized by stating that $h \leqslant 12.8R_p$ requires thickness-corrected formulations of Eq. (5)) are very useful in the discussion of this well-reasoned contact mechanics formulation, but are also arbitrary. That is, this concept of finite polymer film thickness does not immediately impose any general analytical limits over which small film thickness $h$ relative to probe radius $R_p$ implies significant deviation from the Hertzian analysis for a given indentation depth $\Delta$. Rather, the authors point out two separate considerations: the valid application of Hertzian contact requires first that the material actually behaves as a linear, time-independent, elastic solid over the imposed $\Delta$ (which may/not be true for strains and force perturbations greater/less than 10%, depending on the material), and second that the zone of elastic deformation should be confined to regions far from the film/substrate interface. For our probe geometry ($R_p = 50$ nm) and force range ($P_{max} = 3$ nN for PEMs assembled at pH = 6.5, the least compliant PEM considered herein), we find that we sample a maximum contact volume of radius a = 7 nm ($\ll$10% of even the thinnest PEM film) and that the induced maximum axial strain $\varepsilon_{zz}$ on any PEM was less than 33% for $\Delta_{max} = 20$ nm. Thus, although film thickness is an important general consideration in the design and interpretation of contact experiments, we feel that the current application of a sphere-tipped cone to shallow indentation depths in these relatively stiff PEM films is reasonably well-modeled by a simple Hertzian approximation of a semi-infinite solid.

## References

[1] Davies PF, Mundel T, Barbee KA. A mechanism for heterogeneous endothelial responses to flow in vivo and in vitro. J Biomech 1995;28(12):1553–60.

[2] Resnick N, Yahav H, Shay-Salit A, Shushy M, Schubert S, Zilberman LC, et al. Fluid shear stress and the vascular endothelium: for better and for worse. Prog Biophys Mol Biol 2003;81(3):177–99.
[3] Shukla A, Dunn AR, Moses MA, Van Vliet KJ. Endothelial cells as mechanical transducers: effects of cyclic strain on enzymatic activity and organization. Mech Chem Biosys 2004;1(4):279–90.
[4] Simmons CA, Nikolovski J, Thornton AJ, Matlis S, Mooney DJ. Mechanical stimulation and mitogen-activated protein kinase signaling independently regulate osteogenic differentiation and mineralization by calcifying vascular cells. J Biomech 2004;37(10): 1531–41.
[5] Pelham RJ, Wang YL. Cell locomotion and focal adhesions are regulated by substrate flexibility. Proc Natl Acad Sci USA 1997;94(25):13661–5.
[6] Anderson DG, Levenberg S, Langer R. Nanoliter-scale synthesis of arrayed biomaterials and application to human embryonic stem cells. Nat Biotechnol 2004;22(7):863–6.
[7] Berg MC, Yang SY, Hammond PT, Rubner MF. Controlling mammalian cell interactions on patterned polyelectrolyte multilayer surfaces. Langmuir 2004;20(4):1362–8.
[8] Mendelsohn JD, Yang SY, Hiller J, Hochbaum AI, Rubner MF. Rational design of cytophilic and cytophobic polyelectrolyte multilayer thin films. Biomacromolecules 2003;4(1):96–106.
[9] Yang SY, Berg MC, Hammond PT, Rubner MF. Primary hepatocytes and fibroblasts response to polyelectrolyte multilayers with polyacrylamide containing polymers. In: American Chemical Society; 2003.
[10] Dimitriadis E, Horkay F, Maresca J, Kachar B, Chadwick R. Determination of elastic moduli of thin layers of soft material using the atomic force microscope. Biophys J 2002;82:2798–810.
[11] Domke J, Dannohl S, Parak WJ, Muller O, Aicher WK, Radmacher M. Substrate dependent differences in morphology and elasticity of living osteoblasts investigated by atomic force microscopy. Colloids Surf B—Biointerfaces 2000;19(4):367–79.
[12] Engler AJ, Richert L, Wong JY, Picart C, Discher DE. Surface probe measurements of the elasticity of sectioned tissue, thin gels and polyelectrolyte multilayer films: correlations between substrate stiffness and cell adhesion. Surf Sci 2004;570:142–54.
[13] Mermut O, Lefebvre J, Gray D, Barrett C. Structural and mechanical properties of polyelectrolyte multilayer films studied by AFM. Macromolecules 2003;36:8819–24.
[14] Richert L, Engler AJ, Discher DE, Picart C. Elasticity of native and cross-linked polyelectrolyte multilayer films. Biomacromolecules 2004;5(5):1908–16.
[15] Dubreuil F, Elsner N, Fery A. Elastic properties of polyelectrolyte capsules studied by atomic-force microscopy and RICM. Eur Phys J E 2003;12:215–21.
[16] Vinogradova OI, Andrienko D, Lulevich VV, Nordschild S, Sukhorukov GB. Young's modulus of polyelectrolyte multilayers from microcapsule swelling. Macromolecules 2004;37:1113–7.
[17] Yang SY, Mendelsohn JD, Rubner MF. New class of ultrathin, highly cell-adhesion-resistant polyelectrolyte multilayers with micropatterning capabilities. Biomacromolecules 2003;4(4): 987–94.
[18] Yang SY, Rubner MF. Micropatterning of polymer thin films with pH-sensitive and cross-linkable hydrogen-bonded polyelectrolyte multilayers. J Am Chem Soc 2002;124(10):2100–1.
[19] Shiratori SS, Rubner MF. pH-dependent thickness behavior of sequentially adsorbed layers of weak polyelectrolytes. Macromolecules 2000;33(11):4213–9.
[20] Cambrex B. http://www.cambrex.com/content/bioscience/CatNav.oid.510.prodoid.Endo-2media. In; 2005.
[21] Cleveland JP, Manne S, Bocek D, Hansma PK. A nondestructive method for determining the spring constant of cantilevers for scanning force microscopy. Rev Sci Instrum 1993;64(2):403–5.
[22] Johnson KL. Contact mechanics. Cambridge: Cambridge University Press; 1994.
[23] Yoo D, Shiratori SS, Rubner MF. Controlling bilayer composition and surface wettability of sequentially adsorbed multilayers of weak polyelectrolytes. Macromolecules 1998;31(13):4309–18.
[24] Gardel M, Oomen B, Barragan P, Rubner MF, Van Vliet KJ. Manuscript in preparation. 2005.
[25] Bradby R, editor. Comprehensive desk reference of polymer characterization and analysis. Oxford: Oxford University Press; 2003.
[26] Pavoor PV, Bellare A, Strom A, Yang DH, Cohen RE. Mechanical characterization of polyelectrolyte multilayers using quasi-static nanoindentation. Macromolecules 2004;37(13): 4865–71.
[27] Bhattacharya A, Nix W. Int J Sol Struc 1988;24:881–91.
[28] Van Vliet KJ. Nanomechanics of crystalline materials: experiments and computations. Ph.D. Thesis, Cambridge: Massachusetts Institute of Technology; 2002.